

Copyright (to be inserted by the publisher)

Influence of Biaxial Surface Stress on Mechanical Indenting Deformations

Y.-H. Lee^{1†}, J.-I. Jang² and D. Kwon¹

¹School of Materials Science and Engineering, Seoul National University,
Shilim-dong, Gwanak-gu, Seoul 151-744, Korea,

²Frontics, Inc., Research Institute of Advanced Materials, Seoul National University,
Shilim-dong, Gwanak-gu, Seoul 151-744, Korea

Keywords: Residual stress, Instrumented indentation, Contact deformation, Stress directionality

Abstract: A theoretical model has been proposed to assess quantitative residual stress from a stress-induced shift in an indentation curve, but the assumption in this model of equibiaxial surface stress has obstructed its application to real structures in complex stress states. Thus we investigated the influence of non-equibiaxial surface stress on contact deformation through instrumented indentations of a biaxially strained steel plate in order to extend the model to a general surface stress by considering a ratio of two principal stresses.

Introduction

An instrumented indentation technique, developed to characterize the mechanical properties of small-volume materials [1-4], is adopted as a nondestructive stress-measurement method. Surface residual stress causes a shift in the indentation curve [5-9], and this is a crucial clue in stress analysis. Numerous studies [5,6] have attempted to derive an empirical relationship between the residual stress and the contact hardness as estimated from the instrumented indentation curve. However, the alteration of the contact hardness by the elastic residual stress is less than 10% of its value in the unstressed specimen [5], so that using the contact hardness as a residual-stress parameter is dubious. Tsui et al. [7], studying the influences of pre-existing surface stresses on indentation plasticity, reported that hardness was invariant regardless of the applied stress. Suresh and Giannakopoulos [8] defined the contributions of residual stress on plastic deformation as a differential contact stress, but this included a plastic deformation-independent hydrostatic stress. Lee and Kwon [9] explored stress interaction from the viewpoint of shear plasticity and proposed an optimized indentation model. This theoretical model, however, treats the pre-existing surface stress as a simple equibiaxial state, and this impedes its application to complex stress states in actual structures. In this paper we investigate the influence of a non-equibiaxial surface stress on the indentation deformation. The instrumented indentation curves obtained from artificially simulated various stress states on a cross-shaped specimen were analyzed using the model of Lee and Kwon [9].

Experimental details

The API X65 steel plate chosen for the study has elastic modulus 210 GPa, Poisson's ratio 0.3, and yield strength 490 MPa. The 15 mm thick cross-shaped specimen shown in Fig. 1(a) was machined and heat-treated at 600 °C for 2 h for stress relaxation, and then its surface was mechanically ground and polished with 0.5 μm alumina powder. In order to strain the cruciform specimen artificially, a stress-generating apparatus with two independent orthogonal loading axes (cross-sectional view) was designed. The specimen was tightened between the upper and lower jigs and was then biaxially loaded using the straining screws at the specimen ends (see Fig. 1(b)); the straining screws in the

† Corresponding author : uni44@mmrl.snu.ac.kr

upper jig created a tensile strain on the top surface whose magnitude was measured by the strain gages.

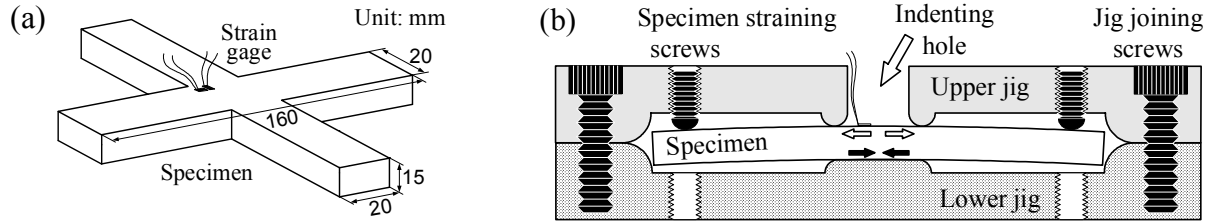


Fig. 1. Schematic diagrams: (a) cruciform specimen and (b) apparatus for artificial straining.

The instrumented indentation tests were carried out using the AIS 3000R system made by Frontics, Inc. whose load and depth resolutions were 0.015 N and 0.1 μm , respectively. A multi-indentation method including loading, unloading and reloading cycles was adopted for the unstressed sample to gather much contact information on different load steps at once. Five indentations were repeated with indentation load steps 98, 196, and 294 N and indentation speed 0.2 mm/min. After testing in the unstressed state, six kinds of surface biaxial strain, including pure shear ($\sigma_x = -\sigma_y \neq 0$), uniaxial ($\sigma_x \neq 0, \sigma_y = 0$), equibiaxial ($\sigma_x = \sigma_y \neq 0$), and biaxial ($\sigma_x \neq \sigma_y \neq 0$) states, were simulated on the specimen using the apparatus in Fig. 1(b). The orthogonal axial strains were converted to applied stresses using Young's modulus and Poisson's ratio. Single indentation tests were performed on the elastically bent specimen inside the indentation hole, where the gradient of the bending strain along the thickness is uniform. The indentation load and testing speed were 294 N and 0.2 mm/min, respectively. The instrumented indentation curves obtained from various biaxial stress states were superposed on that for the unstressed state to assess the shift in the indentation curve.

Results and Discussion

A representative indentation curve for the unstressed sample (solid circles in Fig. 2) was selected from the middle of the raw data. The maximum depth h_{max} at the peak indentation load L_{max} was $68.70 \pm 0.16 \mu\text{m}$. The contact depth was calculated from the unloading part corresponding to each load step using Oliver-Pharr analysis [1]:

$$h_c = h_{\text{max}} - 0.72 \frac{L_{\text{max}}}{S}, \quad (1)$$

where h_c is the contact depth and S is the gradient of the tangent to the unloading curve at the maximum depth. The Vickers contact hardness, calculated by dividing L_{max} by the contact area A_c or $24.5h_c^2$, was $2.85 \pm 0.16 \text{ GPa}$. The load dependency of the contact area is expressed as $A_c = L/H$ regardless of the stress state because hardness is independent of the elastic surface stress, according to previous research [7-9].

Two orthogonal stress components σ_x and σ_y created on the specimen are related to each other by a stress ratio κ or σ_y/σ_x ; the pure shear, uniaxial, and equibiaxial stress states correspond to κ values of -1.0 , 0 , and $+1.0$, respectively (see Table 1). The instrumented indentation curves from biaxially stressed states are superposed on that of the unstressed state in Fig. 2. The stress-induced shift of the indentation load in the stressed state is explained as follows: the increase in the shear stress under tensile stress enhances indentation plasticity, thereby producing a lower indentation load than in the unstressed state. The amount of the shift in the indentation curve of the equibiaxial state from the unstressed state was about twice that of the uniaxially stressed state. While the curve shift in the

pure-shear state is negligible, the amount of the stress-induced load shift is linearly proportional to the applied average stress because the averaged effects of the surface biaxial stress are transmitted along a unique indenter column.

Table 1. Artificially applied stress states on the cruciform specimen.

	Axial stress components [MPa]		Stress ratio κ	Fitted loading curve
	σ_x (major)	σ_y (minor)		
State #1	-415	-414	1.0 (equibiaxial)	$L = 0.173h^{1.78}$
State #2	-375	-248	0.66 (biaxial)	$L = 0.162h^{1.79}$
State #3	-408	0	0 (uniaxial)	$L = 0.196h^{1.74}$
State #4	-239	231	-0.97 (pure-shear)	$L = 0.146h^{1.80}$
State #5	414	0	0 (uniaxial)	$L = 0.132h^{1.81}$
State #6	428	427	1.0 (equibiaxial)	$L = 0.116h^{1.83}$
Stress-free	-	-	-	$L = 0.175h^{1.75}$

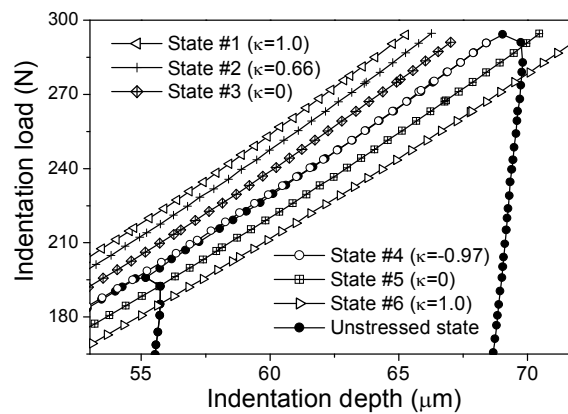


Fig. 2. Superposed indentation curves of the artificially stressed and unstressed states.

In order to analyze the load shifts in Fig. 2 using the model in [9] for surface equibiaxial stress, equivalent equibiaxial states ($\sigma_x^{\text{avg}} = \sigma_y^{\text{avg}} = (1 + \kappa)\sigma_x / 2$) were extracted from the created biaxial stresses by averaging two orthogonal axial components. In the model in [9], the equivalent equibiaxial state was decomposed into a mean stress plus a plastic-deformation-sensitive shear deviator stress σ^D . The stress-induced load shift was defined as a residual-stress-induced normal load L_{res} and was expressed as a product of the deviator-stress component parallel to the indentation axis $\sigma_{zz}^D = -(1 + \kappa)\sigma_x / 3$ and the contact area A_C . Reversible recoveries of the contact deformation during depth-controlled stress relaxation were expressed as an integral equation [9]. In order to solve this equation, the applied stress was assumed to relax linearly and the response of A_C was expressed as L/H . Thus a final equation for the equivalent equibiaxial stress was found as Eq. (2) using the contact area of the tensilely stressed state A_C^T :

$$\sigma_{\text{indent}}^{\text{avg}} = -\frac{3 L_{\text{res}}}{2 A_C^T}. \quad (2)$$

The stress values $\sigma_{\text{indent}}^{\text{avg}}$ from Eq. (2) are compared with the applied average stress $\sigma_{\text{appl}}^{\text{avg}}$ in Table 2 and show good agreement within a standard deviation of ± 10.7 MPa. Two orthogonal stress

components were also calculated from the average stress estimated by the indentation model and κ value; the major principal stress component σ_x was calculated from $2\sigma_{\text{indent}}^{\text{avg}}/(1+\kappa)$, and the minor principal stress component σ_y by multiplying κ to the predetermined σ_x . The recalculated stress components in Table 2 also showed good agreement with the applied stress components in Table 1, except for the result for the pure-shear stress state. The large stress discrepancy in the pure-shear state was attributed to the negligible value of the stress-induced load shift (see Fig. 1) and the low sensitivity of the instrumented indentation technique to the small average stress near zero.

Table 2. Stresses estimated from the indentation model and from the strain gage.

	Average stress, $\sigma_{\text{indent}}^{\text{avg}}$ [MPa] (strain gage measure)	Average stress, $\sigma_{\text{appl}}^{\text{avg}}$ [MPa] (instrumented indentation model)	σ_x component [MPa]	σ_y component [MPa]
State #1	-414.5	-407.8 ± 21.5	-408.3 ± 21.5	-407.3 ± 21.4
State #2	-311.5	-303.3 ± 29.8	-365.1 ± 35.8	-241.5 ± 23.7
State #3	-204.0	-187.4 ± 14.8	-374.7 ± 29.5	0 ± 0
State #4	-4.0	-2.7 ± 36.5	-160.8 ± 2178.2	155.5 ± 2105.3
State #5	207.0	205.3 ± 53.1	410.6 ± 106.2	0 ± 0
State #6	427.5	411.6 ± 74.0	412.1 ± 74.1	411.1 ± 73.9

Summary

Instrumented indentation tests carried out on an artificially stressed cruciform specimen produced significant shape shifts in the indentation curves from that of the unstressed sample. The shift or difference in the indentation load in the stressed and unstressed states can be analyzed using an indentation model developed for the equibiaxial stress state. To do this, equivalent equibiaxial states were extracted from the created biaxial stresses by averaging two orthogonal axial stresses. The average stresses from the proposed indentation model agreed well with the applied average stresses. In addition, two principal stress components were calculated from the predetermined average stress by using the stress ratio κ .

References

- [1] W.C. Oliver and G.M. Pharr: J. Mater. Res. Vol. 7 (1992), p. 1564.
- [2] J. Mencik and M.V. Swain: Mater. Forum, Vol. 18 (1994), p. 277.
- [3] J.-H. Ahn and D. Kwon: J. Mater. Res. Vol. 16 (2001), p. 3170.
- [4] Y.-H. Lee and D. Kwon: Key Eng. Mater. Vol. 161-163 (1999), p. 569.
- [5] G. Sines and R. Calson: ASTM Bulletin, February (1952), p. 35.
- [6] A.V. Zagrebelny and C.B. Carter: Scripta Mater. Vol. 37 (1997), p. 1869.
- [7] T.Y. Tsui, W.C. Oliver and G.M. Pharr: J. Mater. Res. Vol. 11 (1996), p. 752.
- [8] S. Suresh and A.E. Giannakopoulos: Acta Mater. Vol. 46 (1998), p. 5755.
- [9] Y.-H. Lee and D. Kwon: Scripta Mater. Vol. 49 (2003), p. 459.